Q/U Imaging ExperimenT (QUIET): a ground-based probe of cosmic microwave background polarization

Immanuel Buder for the QUIET Collaboration

Department of Physics, U. of Chicago, 933 E. 56th St., Chicago, IL USA 60637

ABSTRACT

QUIET is an experimental program to measure the polarization of the Cosmic Microwave Background (CMB) radiation from the ground. Previous CMB polarization data have been used to constrain the cosmological parameters that model the history of our universe. The exciting target for current and future experiments is detecting and measuring the faint polarization signals caused by gravity waves from the inflationary epoch which occurred $< 10^{-30}$ s after the Big Bang. QUIET has finished an observing season at 44 GHz (Q-Band); observing at 95 GHz (W-Band) is ongoing. The instrument incorporates several technologies and approaches novel to CMB experiments. We describe the observing strategy, optics design, detector technology, and data acquisition. These systems combine to produce a polarization sensitivity of 64 (57) μK for a 1 s exposure of the Phase I Q (W) Band array. We describe the QUIET Phase I instrument and explain how systematic errors are reduced and quantified.

Keywords: QUIET, cosmic microwave background, cosmology observations, instrumentation: polarimeters

1. INTRODUCTION

QUIET is an experimental program to measure the polarization anisotropy of the Cosmic Microwave Background (CMB). In the last few years, increasingly precise measurements[1–4] of the polarization have helped both to verify the standard cosmological model and to provide some constraints on cosmological parameters. The polarization of the CMB is uniquely sensitive to primordial gravity waves, which create characteristic degree scale divergence free polarization patterns on the sky known as B-modes. Primordial gravity waves are generically predicted by inflationary models, and a measurement of their amplitude would constrain the energy scale of inflation[5] and provide information about the physics of inflation. The currently deployed QUIET Phase I makes precise measurements of the CMB polarization at angular scales $25 \lesssim \ell \lesssim 1000$; however, it will not have the sensitivity necessary to detect B-modes. QUIET Phase II, now being planned based on the success of Phase I, will have the sensitivity to detect B-modes or place a stringent limit on their amplitudes. Because CMB polarization, and B-modes in particular, are extremely faint, measuring them requires low instrumental noise and immunity from systematic effects which can create spurious polarization. These requirements can be met in a variety of ways. QUIET chooses to do so by observing from the ground, using the sky rotation and rotation about the telescope optical axis to modulate the polarization signal. The unique High Electron Mobility Transistor (HEMT) based detector modules both form the core of the low noise detector system and allow additional electronic modulation by high frequency switching of the polarization signal. A brief overview of QUIET Phase I is given in Sec. 2, with details in the following sections. Measurements and estimates of systematic effects are given in Sec. 9. In Sec. 10 we conclude with an outlook for results from QUIET Phase I and our plans for QUIET Phase II. Other details about QUIET can be found elsewhere.[6–10]

2. OVERVIEW

This section provides an overview of the QUIET Phase I experiment (and hereafter "QUIET" will refer to QUIET Phase I unless otherwise noted). QUIET collects science data from the Chajnantor observing site (see Sec. 3) in Chile. CMB photons are collected by a 1.4 m Mizuguchi-Dragone telescope.[11–14] Beams for each detector are formed by a feedhorn array.[15] At the end of each feedhorn, the radiation enters a septum polarizer that splits it into two circularly polarized components. The telescope, feedhorns, and septum polarizers are

Send correspondence to ibuder@uchicago.edu, 1 773 702 1893

further described in Sec. 4. The feedhorns, septum polarizers, and detectors are housed in a cryostat, described in Sec. 5. The detectors are HEMT-based polarimeter modules (see Sec. 6) which convert the two circular polarization components into a measurement of the Stokes linear polarization parameters Q and U. The 44 GHz (Q-Band) array has 19 such modules, and the 95 GHz (W-Band) array has 90 modules, making it the largest such array yet deployed. The electronics necessary to bias and readout the detector modules are described in Sec. 7. The electronics are controlled by higher level software which is described in Sec. 8. Characterization of the complete QUIET system, measurements, and estimates of systematic effects are given in Sec. 9. Figure 1 shows a schematic and a picture of the QUIET instrument.

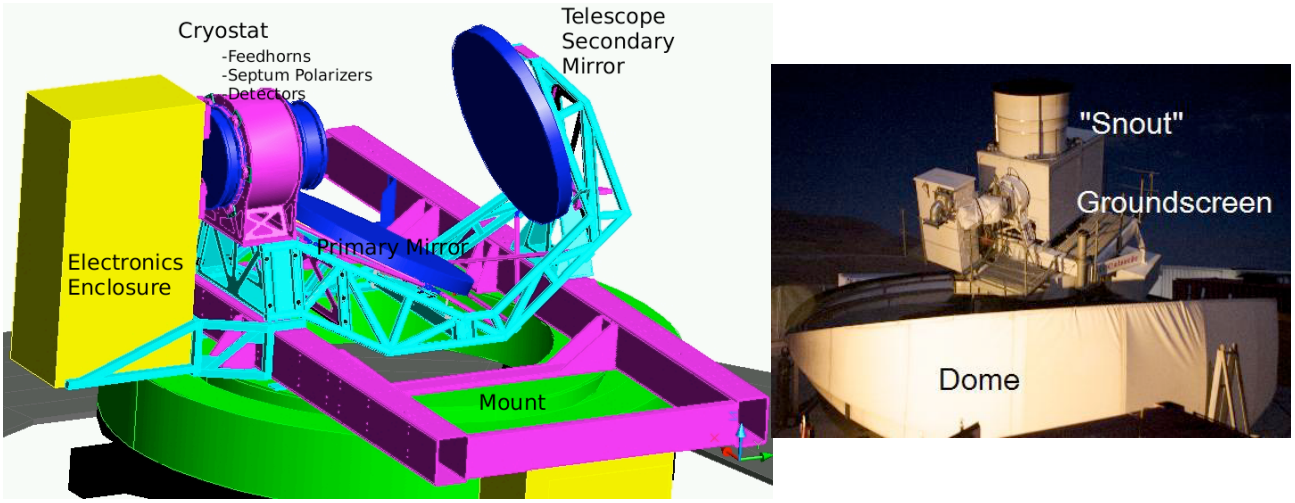

Figure 1. Left: Schematic diagram of the QUIET instrument. Right: Photo of it deployed in Chajnantor. The mount, telescope, and groundscreen are described in Sec. 4, the cryostat is described in Sec. 5, and the electronics are described in Sec. 7.

3. SITE AND OBSERVING SUMMARY

QUIET observes from the Chajnantor Plateau, located at 5080 m elevation in the Atacama Desert, Chile. The elevation and the aridity make it an excellent site for microwave astronomy.[16–18] The site is accessible year-round, which simplifies logistics.

QUIET began science observing in October 2008 with the Q-Band array. In June 2009, Q-Band observation finished, and the W-Band array was installed. W-Band science observations began in August 2009 and are ongoing. The two arrays are installed on the same telescope and mount, but have separate cryostats, detectors, and electronics. Any significant differences between the two arrays will be noted in the following sections. Both arrays observe the same four patches for CMB data and two patches for galactic science data (see Table 1 and Fig. 2). With the site latitude of 23°S and our choice of patches, each patch rises and sets as the sky rotates. This rotation modulates the polarization signal because a fixed sky polarization enters into different combinations of the detector polarization axes. The weekly rotation of the telescope about its optical axis ("boresight rotation") provides additional modulation. Each patch is scanned with a periodical azimuth motion at fixed elevation for ∼1.5 hours until it drifts out of the line of sight. The elevation and azimuth are then changed to recenter the patch, and this process continues until the patch sets and another patch is selected. Each change in elevation is followed by a "mini sky dip," a small amplitude elevation scan. The signal caused by the changing effective atmosphere temperature is used for responsivity calibration.[10]

During the Q-Band season we achieved 66% observation efficiency, taking 3650 hours of astronomical observation data. Of that total, ∼10% are devoted to calibration, using astronomical sources. Table 1 lists the amount of time spent on each patch and the measurements obtained from each calibrator. As of this writing, the W-Band season includes more than 3000 hours of observation, and an additional 4500 are expected by the end of 2010. A similar fraction of W-Band observing is used for calibration.

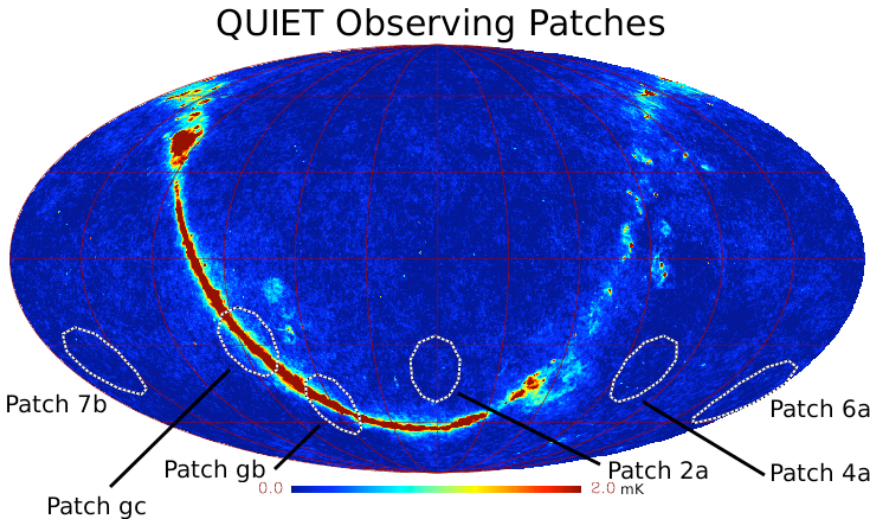

Figure 2. The four QUIET CMB patches and two galactic science patches projected in equatorial coordinates. The CMB patches were chosen to minimize contamination from astronomical foregrounds. The background is the WMAP Q-Band temperature map.

Table 1. Summary of QUIET Q-Band observations. The observing time is allocated similarly in W-Band. Each CMB or galactic science patch is $\sim 15^\circ \times 15^\circ$. The coordinates of the center of each patch are given in (RA, DEC).

Observation target	Observing time (hours)	Science or calibration obtained
Patch 2a (181, -39)	1000	CMB science
Patch 4a (78, -39)	750	CMB science
Patch 6a (12, -48)	900	CMB science
Patch 7b (341, -36)	300	CMB science
Patch gb (240, -53)	300	Galactic science
Patch gc (266, -29)	100	Galactic science
Jupiter	20	responsivity, pointing, beam shape
Tau A	50	responsivity, beam shape, detector polarization angles
Moon	30	responsivity, pointing, detector polarization angles, temperature to polarization leakage
Sky dip	200	responsivity, temperature to polarization leakage

4. TELESCOPE AND OPTICS

The QUIET telescope is a 1.4 m Mizuguchi-Dragone reflector.[11–14] The two mirrors are aluminum, the backs of which are lightweighted and connected by adjustable hexapods to the steel support structure. Both mirrors are enclosed by a comoving, ambient temperature eccosorb-lined ground screen. Until January 2010, the top aperture of the ground screen did not block the "triple-reflection" sidelobe,* which was known from simulation of the design. Thereafter, the "snout" which was part of the original groundscreen design was installed on the top of the groundscreen. Beam maps conducted with an impact ionization avalanche transit-time (IMPATT) source before and after the installation of the snout confirm that the sidelobe was reduced by several orders of magnitude.

The optical beam of each detector module is formed by a corrugated, linear flare feedhorn. These feedhorns are constructed as a "platelet array." Large plates are machined so that each plate forms a slice of all the feedhorns, transverse to the optical axis. The plates are then stacked along the optical axis and diffusion bonded together to form a single component containing all the feedhorns.[15] The platelet design incorporates lightweighting holes that also function as access holes for attachment screws. The fabrication costs of these arrays are at least an order of magnitude less than for the same number of electroformed feedhorns. Measurements of the return loss and beam characteristics of the platelet arrays show performance comparable to an equivalent electroformed design and in accordance with theoretical predictions.

Light exits each feedhorn into a septum polarizer,[19] which separates the left and right circularly polarized components required as the inputs to the QUIET detector modules. A bandpass mismatch between the Q-Band septum polarizers and modules resulted in a systematic temperature to polarization leakage effect of order 1%, the consequences of which are addressed in Sec. 9. This systematic effect is not present in W-Band, and the corresponding leakage effects are typically <1%. The septum polarizers of two of the 19 Q-Band (six of the 90 W-Band) modules are replaced by assemblies of orthomode transducers (OMTs) and magic tees that make the modules sensitive to CMB temperature rather than polarization anisotropies. Such modules are referred to as "TT modules."

All of the above components, as well as the cryostat and electronics described below, are installed on the former CBI mount system.[20] This provides three-axis motion including the boresight rotation described in Sec. 3. The azimuth axis is capable of scanning at 6°/s with a typical scan frequency of 100 mHz. This scan modulates the CMB signal at a higher frequency than the detector and atmospheric 1/f noise.

5. CRYOSTAT

The platelet array, septum polarizers, and detector modules in each array (Q-Band or W-Band) are mounted inside and supported by a cryostat. Light enters the cryostat through an ultra-high molecular weight polyethylene window with an expanded-Teflon anti-reflection coating. With this coating the loss through the window is at the percent level for microwave frequencies. Infrared radiation is blocked by a styrofoam filter, reducing thermal loading on the cold stage. The cold stage containing the detectors and optical components is cooled to 20 K (25 K for W-Band) for optimal noise performance by two CTI 1020 Gifford-McMahon refrigerators. Silicon diode thermometers on the detectors, platelet array, refrigerator heads, and secondary 80 K stage continuously monitor the cooling and temperature regulation performance. Stycast epoxy sealed hermetic pass-throughs allow the bias and readout lines for the detectors, described in the next section, to be brought out of the cryostat. Figure 3 shows the W-Band cryostat.

6. DETECTORS

The QUIET detectors are miniaturized pseudo-correlation polarimeter "modules." Each module is based on HEMT amplifiers. Previous experiments including WMAP,[21] DASI,[22] CBI,[20] PIQUE,[23] and CAPMAP[24] also used HEMT-based polarimeters, but QUIET is part of a new generation that takes advantage of breakthroughs in millimeter-wave circuit technology and packaging[25] to replace waveguide-block components and connections

*This sidelobe is caused by the edge of the beam coming from the primary mirror impinging on the top edge of the secondary mirror. This third reflection results in a far sidelobe ∼50°away from the main beam.

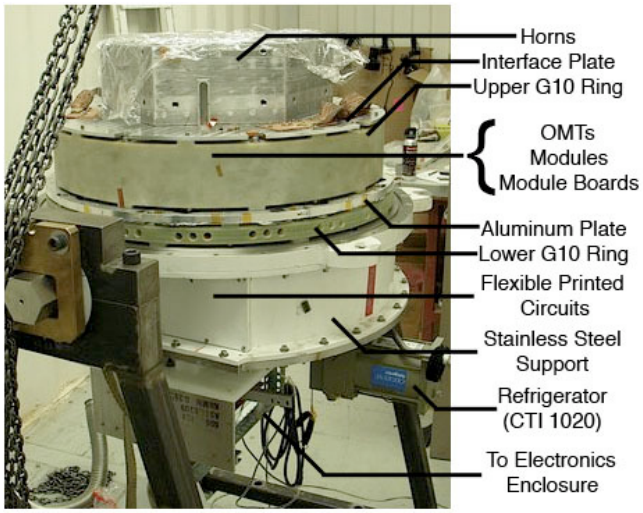

Figure 3. The W-Band cryostat and some of its components. Including the outer sections not shown, its dimensions are 71 cm×66 cm. The Q-Band cryostat is 71 cm×71 cm. The AIBs (see Sec. 7) are mounted on the metal structure attached at the bottom.

with strip-line coupled devices. The resulting modules are 5.1 cm×5.1 cm for Q-Band (3.2 cm×2.9 cm for W-Band), almost an order of magnitude smaller than a comparable waveguide design. Figure 4 shows a photograph of a W-Band module and a diagram representing the signal processing.

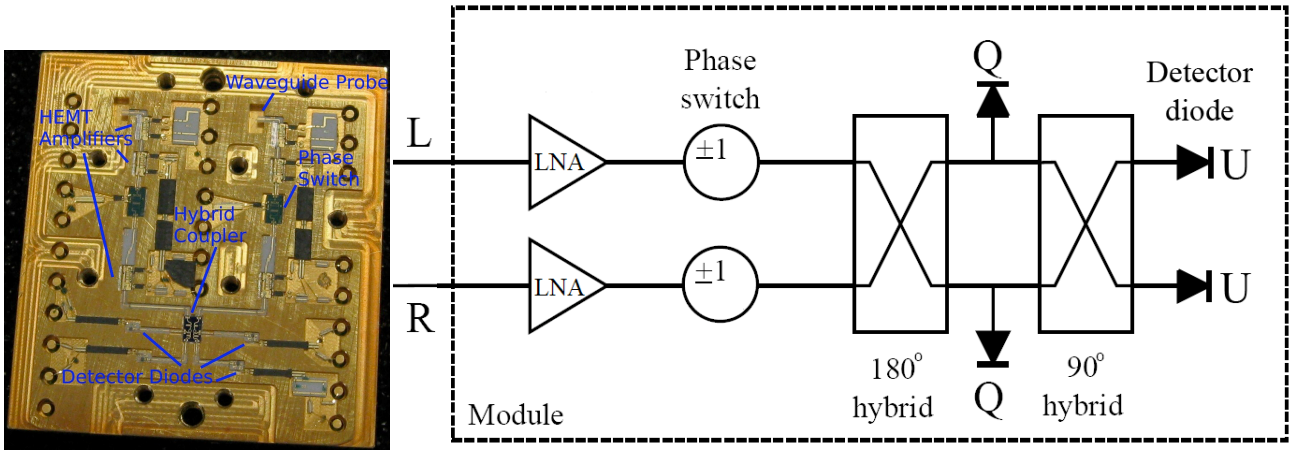

Figure 4. Left: Photograph of the inside of a W-Band module, 3.2 cm×2.9 cm. Right: A conceptual schematic of the signal flow in a QUIET module. Left and right circularly polarized modes are represented by "L" and "R." They are amplified by HEMT-based low noise amplifiers, "LNA." Phase switches, "±1," provide electronic modulation. Detector diodes, "Q" and "U," measure both linear polarization components.

The module takes two inputs, left and right circularly polarized modes, from the septum polarizer. Each input is fed by a waveguide probe into a chain (hereafter "leg") of HEMT amplifiers. Each leg contains a phase switch which can modulate the signal at 4 kHz or 50 Hz. After amplification and modulation, the signals are combined in a 180° hybrid coupler. Two of the outputs of this coupler are rectified by two detector diodes, designated Q1 and Q2. Each diode measures E_x^2 or E_y^2, where E_i is the component of the electric field in the i direction. The phase switch modulation causes $x \leftrightarrow y$ so that the difference of the two states is a measurement of the Q linear polarization component. The other two outputs of the hybrid coupler continue into a second 90° coupler so that two diodes, designated U1 and U2, measure the orthogonal U polarization component. This

simultaneous measurement of Q and U in each module is one of the unique features of the QUIET design. The 4 kHz modulation of each polarization measurement is faster than the 1/f knee frequency of the amplifier noise and atmospheric fluctuations.

The 4 kHz modulation in one leg is sufficient to suppress the effects of amplifier gain and atmospheric fluctuations. The additional 50 Hz modulation of the phase switch in the other leg suppresses spurious instrumental polarization that might otherwise be caused by transmission differences between the two phase states in either of the two phase switches. This double demodulation does not degrade the detector sensitivity and, in combination with our other modulation techniques, keeps the optical chain simple by eliminating the need for polarization modulation by optical components and their associated systematic effects.

One consequence of the modules' integrated circuit-style design is that they can be mass produced and tested for performance and to ensure quality control using techniques adapted from the semiconductor industry. The W-Band array pictured in Fig. 5 with 90 modules is the largest HEMT-based array yet deployed. One technique necessary for its deployment is the optimization procedure whereby the biasing is adjusted to achieve the best noise performance for each module. This procedure exploits the ∼10 amplifier biasing degrees of freedom and optimizes the signal to noise ratio using a rotating sparse wiregrid as polarization signal source. This method can optimize the full W-Band array in less than 24 hours, and we expect it to be a useful technique for future large polarimeter arrays. Further details about the QUIET polarimeter modules are provided in Cleary et al., 2010.[8]

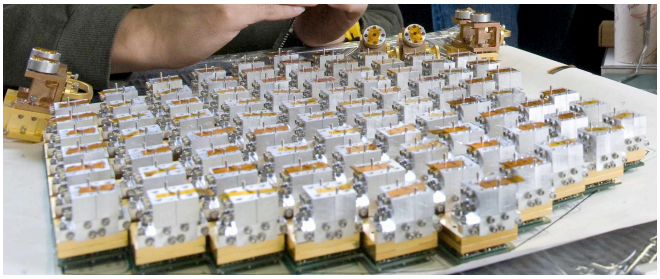

Figure 5. The 90-element W-Band array under assembly. An aluminum septum polarizer is attached to each gold-plated brass module.

7. DETECTOR BIAS AND READOUT ELECTRONICS

The modules are mounted on custom module assembly board (MAB) circuit boards which provide the electrical connection for module bias and readout as well as protection circuitry. Each MAB supports seven modules as shown in Fig. 6. This grouping of modules into sets of seven simplifies system integration. From the MAB, bias and readout signals travel on high density flexible printed circuits (FPCs) which bring them out of the cryostat. Each FPC carries ∼30 independent signal lines and thermally isolates the cold stages inside the cryostat from the warm electronics. The warm ends of the FPCs connect to array interface boards (AIBs) mounted on the back of the cryostat (see Fig. 3) which provide additional protection for the modules against undesired voltages or currents. From the AIBs, signals travel along shielded ribbon cable to custom circuit boards in a VME crate for biasing, amplification, and digitization inside a thermally regulated electronics enclosure (see Fig. 1).

As discussed in Sec. 6, each module has ∼10 tunable biases. Each of these biases is controlled by a 10-bit DAC, which provides the necessary range and precision to optimize the performance of each module. The output of each module detector diode is amplified by ∼100 before digitization. Digitization is performed by custom 32-channel ADC boards[26] based on the Analog Devices AD7674 18-bit ADC. Each channel is sampled at 800 kHz, allowing the differentiation ("demodulation") of the 4 kHz phase states which reconstructs the polarization signal to be performed by an FPGA on each ADC board. Each ADC receives the same 4 kHz and 50 Hz modulation signals sent to the phase switches so that the FPGA can assign each data sample the proper modulation phase. Moreover, the FPGA "blanks" 14% of the samples nearest the phase switch transitions so that these periods when the signal level is unstable do not contaminate the data. Although the full 800 kHz data can be acquired for

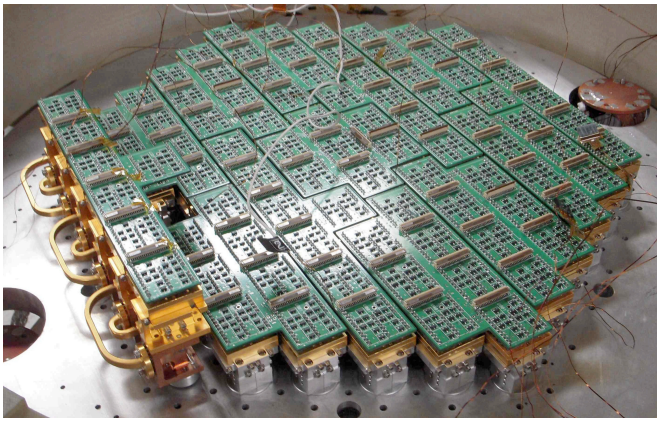

Figure 6. W-Band array with MABs attached. Each MAB mounts seven modules. Thirteen such MABs of five shapes comprise the W-Band array. The six modules on the left are the TT modules. The feedhorns point downward, but are not visible here.

diagnostic and monitoring purposes, normally only two (three for W-Band) 100 Hz data streams are recorded for each diode. In the "average" stream, each 800 kHz sample is summed, regardless of its phase switch modulation state. The average stream corresponds to the total radiation power level incident on the detector and is important for monitoring purposes, but is insensitive to polarization. In the "demodulated" stream, samples are differenced according to their phase switch state; this is the polarization-measuring data that are normally used for analysis. In the "quadrature" stream, recorded only in W-Band, samples are differenced 90° out of phase with the 4 kHz phase state switching. The quadrature data have the same noise as demodulated data, but no signal. The quadrature data are used to monitor potential contamination and understand the detector noise properties.

In addition to the data readout and monitoring, a custom housekeeping system monitors the HEMT biases, cryostat temperature, cryostat vacuum pressure, warm electronics temperature, and ambient humidity. These monitoring data are collected at 1 Hz. Digital clocks are generated by and the data acquisition timing is synchronized by a Symmetricom TTM635VME-OCXO time-code reader. The various data streams and monitoring data are integrated and recorded by the software described in the next section.

8. SOFTWARE AND DATA MANAGEMENT

The QUIET data acquisition and control software uses a modular architecture to coordinate the independent systems composing QUIET. At the lowest level, data are transferred to and from the ADC FPGAs by a VME computer running a custom real-time program. This program implements the synchronous requirements of control and readout so higher level components need only communicate with it asynchronously via standard ethernet interfaces. One such component is responsible for collecting the 100 Hz detector data and integrating it with other independently collected monitoring data such as the cryostat pressure and ambient humidity. All monitoring data are downsampled and displayed on a continuously updating website that can be viewed both by local observers and by the collaboration worldwide, via the internet. The full data rate (∼8 GB/day, ∼five times more for W-Band) is written to disk in the site control room. The data are sent to the U.S. weekly on DVD (Blu-ray for W-Band) and mirrored to the analysis centers in Chicago, Oslo, and KEK. A subset (∼10%) of the data is transferred every day by internet for more rapid analysis and monitoring. An SQL database is maintained so that each data file can be tracked as it is transferred and processed. It is also indexed by observation so that the data corresponding to a particular observation can be easily located. Figure 7 shows a diagram of the control software and data flow.

9. CHARACTERIZATION AND SYSTEMATIC EFFECTS

As discussed in Sec. 3, ∼10% of the observing time is used for calibration. The beam shape, telescope pointing, detector responsivity, detector polarization angles, and magnitude of temperature to polarization leakage effects

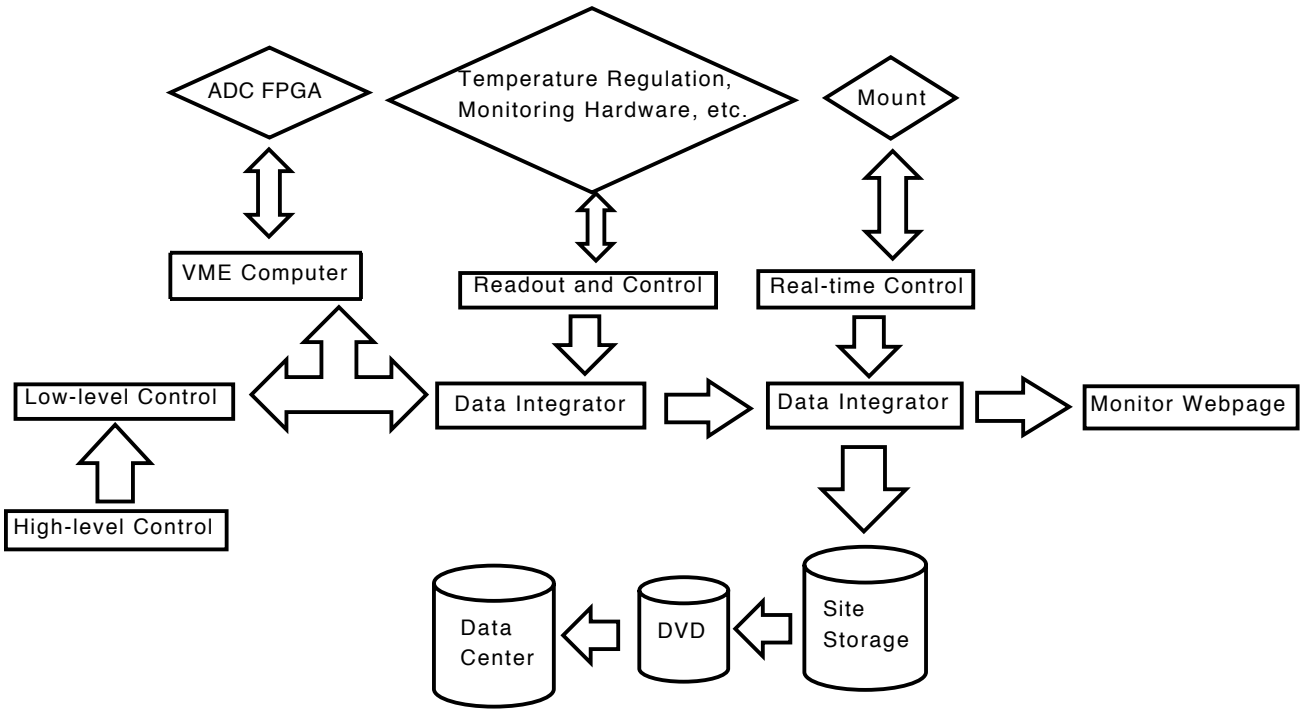

Figure 7. Diagram of QUIET control and readout software showing major components. Diamonds indicate hardware components, rectangles software, and cylinders storage, respectively.

are obtained from these calibration measurements. Some results for Q-Band are listed in Table 2. More details about the beam calibration can be found in Monsalve et al., 2010[9] and about responsivity calibration in Dumoulin et al., 2010.[10] The CMB science data are used to measure the detector 1/f knee frequency and sensitivity performance. Typical knee frequencies for polarization-sensitive demodulated data are ≈20 mHz. The combined array sensitivity achieved during Q-Band observation is $64 \pm 8\ \mu\mathrm{K}\sqrt{s}$; the W-Band sensitivity achieved to date in the field is $57 \pm 14\ \mu\mathrm{K}\sqrt{s}$.[†] We take the noise correlation among the detectors into account in our noise model. As explained in Jarosik et al., 2003[21] a difference in power between the two legs in a module causes the white noise of different detector diodes to be correlated. We measure this correlation for each CMB patch observation and find the correlation coefficients to be stable throughout the season in accordance with our understanding of the noise. The typical knee frequency is much less than the typical azimuth scan frequency of 100 mHz so the detector 1/f noise does not significantly degrade the sensitivity.

The uncertainty in our calibration and instrumental systematic effects can produce biases in the CMB angular power spectrum result. We simulate the most important effects and show that they are negligible and well below the statistical error from noise in the power spectrum. The temperature to polarization leakage effect described in Sec. 4 could cause a fake polarization signal proportional to the unpolarized CMB temperature anisotropy. However, this small leakage is further reduced by our observing strategy, which combines sky rotation and boresight rotation to frequently rotate the detector polarization axes. Simulations show that the residual effect is negligible compared to the error from statistical noise expected in Q-Band for Phase I, even without correction using the measured leakage coefficients. Similar leakage effects can be created by the telescope optics; however, simulations of the design and measured optics leakages[9] both show that these leakages are negligible as well. We perform similar simulations to estimate the impact of uncertainty in calibration. We use the uncertainty from calibration measurements of the beam shape, telescope pointing, relative detector responsivity, and polarization

[†]The absolute responsivity, measured with Tau A, is needed to normalize the sensitivity. The uncertainty is dominated by the uncertainty in the Tau A polarization fraction.

Table 2. Summary of QUIET calibration. Results are for Q-Band. Values are preliminary.

	Uncertainty	Typical Value
Beam width (FWHM)	<0.1 arcmin	27 arcmin
Beam ellipticity	0.6%	1.5%
Telescope pointing	4 arcmin	-
Polarization responsivity	7%	2 mV/K
TT module responsivity	5%	2 mV/K
Detector polarization angles	$\pm 2^\circ$	-
Temperature to polarization leakage	± 0.5 dB	-20 dB (-27 dB for "U" diodes)

angles to simulate the propagated systematic uncertainties in the CMB power spectrum. In all cases these are less than the uncertainty due to detector noise, usually by an order of magnitude or more. Although the analysis is not complete, we have already simulated and quantified what are expected to be the most significant systematic effects. As a demonstration of the instrument and our understanding, Figure 8 shows a polarization map of one of our galactic science patches along with a WMAP map for comparison.

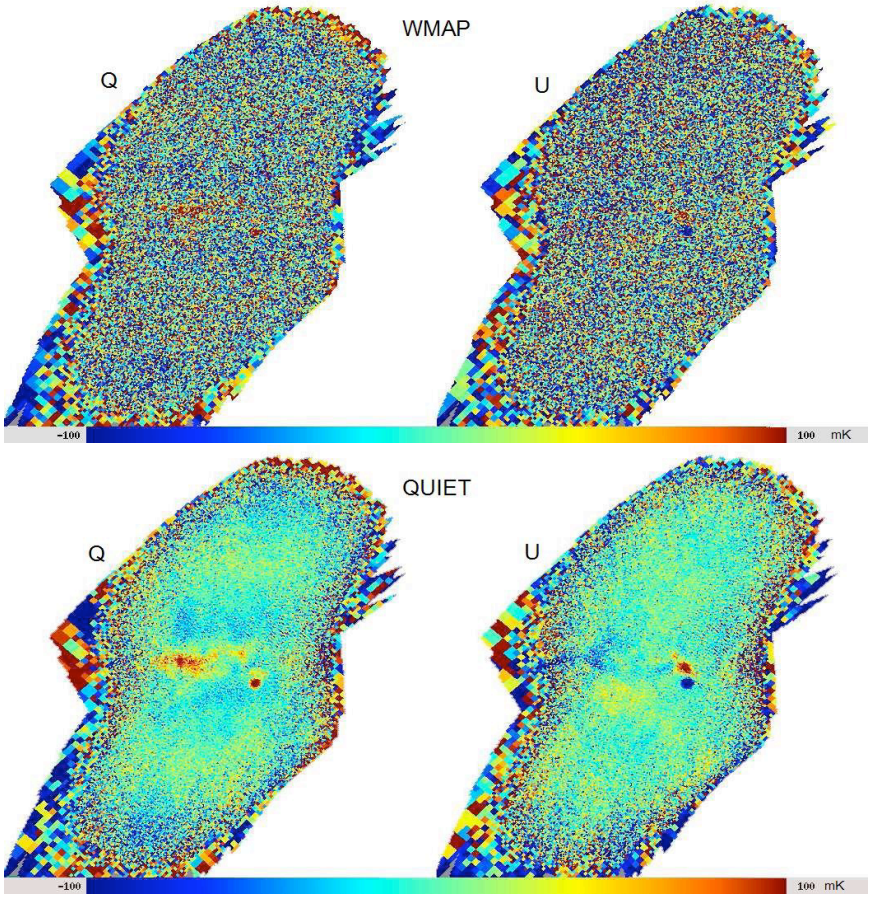

Figure 8. Preliminary map of galactic science patch gb ($\sim 15^\circ \times 15^\circ$) from ~100 hours of QUIET (bottom) and ~200 hours of WMAP5 (top) Q-Band data. The QUIET map shows much better sensitivity.

10. CONCLUSION

QUIET Phase I has successfully deployed two polarization sensitive HEMT-based radiometer arrays, the W-Band array being the largest such array yet. We have characterized both arrays in the field and the measured sensitivities of 64 and 57 $\mu K\sqrt{s}$ will yield a competitive measurement of the CMB polarization. Analysis of the Q-Band data is underway, and the most important systematic effects and calibration uncertainties are shown not to impact the result. W-Band observation continues with the expectation to make an even more sensitive measurement. Having demonstrated our choice of instrument technologies and techniques, we are planning QUIET Phase II, which will deploy an order of magnitude more modules to make measurements at 32, 44, and 95 GHz. The expected sensitivity of these ∼1600 modules will be sufficient to detect B-modes from primordial gravity waves or to place a stringent limit on the tensor-to-scalar ratio which parameterizes them at $r \simeq 0.01$.

ACKNOWLEDGMENTS

Support for the QUIET instrument and operations comes through the NSF cooperative agreement AST-0506648. Support also provided by AST-04-49809, PHY-0355328, DE-AC02-05CH11231, JSPS KAKENHI (A) 20244041, and by the Strategic Alliance for the Implementation of New Technologies (SAINT). We are particularly indebted to the engineers who maintained and operated the telescope: J. Cortes, C. Jara, F. Munoz, and C. Verdugo. Immanuel Buder acknowledges support from a Department of Education GAANN Fellowship.

REFERENCES

[1] Sievers, J. L. et al., "Implications of the Cosmic Background Imager Polarization Data," *Astrophys. J.* **660**, 976–987 (2007).

[2] Bischoff, C. et al., "New Measurements of Fine-Scale CMB Polarization Power Spectra from CAPMAP at Both 40 and 90 GHz," *Astrophys. J.* **684**, 771–789 (2008).

[3] Brown, M. L. et al., "Improved measurements of the temperature and polarization of the CMB from QUaD," *Astrophys. J.* **705**, 978–999 (2009).

[4] Chiang, H. C. et al., "Measurement of CMB Polarization Power Spectra from Two Years of BICEP Data," *Astrophys. J.* **711**, 1123–1140 (2010).

[5] Bird, S., Peiris, H. V., and Easther, R., "Fine-tuning criteria for inflation and the search for primordial gravitational waves," *Phys. Rev.* **D78**, 083518 (2008).

[6] Newburgh, L. et al., "Measuring CMB Polarization with QUIET: The Q/U Imaging ExperimenT," *to appear in Proceedings of the Twelfth Marcel Grossmann Meeting on General Relativity* (2010).

[7] Kusaka, A. et al., "The QUIET experiment," *to appear in Proceedings of the 45th Rencontre de Moriond* (2010).

[8] Cleary, K. A. et al., "Coherent polarimeter modules for the QUIET experiment," *Proc. SPIE* **7741** (2010). To appear.

[9] Monsalve, R. et al., "Beam characterization for the QUIET Q-Band instrument using polarized and unpolarized astronomical sources," *Proc. SPIE* **7741** (2010). To appear.

[10] Dumoulin, R. N. et al., "Responsivity Calibration of the QUIET Q-band Array," *Proc. SPIE* **7741** (2010). To appear.

[11] Mizugutch, Y., Akagawa, M., and Yokoi, H., "Offset dual reflector antenna," *IEEE Antennas and Propagation Society International Symposium* **14**, 2–5 (1976).

[12] Dragone, C., "Offset multireflector antennas with perfect pattern symmetry and polarization discrimination," *Bell Syst. Tech. J.* **57**, 2663–2684 (1978).

[13] Hanany, S. and Marrone, D. P., "Comparison of designs of off-axis gregorian telescopes for millimeter-wave large focal-plane arrays," *Applied Optics* **41**, 4666–4670 (2002).

[14] Tran, H., Lee, A., Hanany, S., Milligan, M., and Renbarger, T., "Comparison of the crossed and the Gregorian Mizuguchi-Dragone for wide-field millimeter-wave astronomy," *Applied Optics* **47**, 103–109 (2008).

[15] Gundersen, J. and Wollack, E., "Millimeter Wave Corrugated Platelet Feeds," *Journal of Physics: Conf. Ser.* **155**, 012005 (2009).

[16] Radford, S. J. E. and Holdaway, M. A., "Atmospheric Conditions at a Site for Submillimeter Wavelength Astronomy," *Proc. SPIE* **3357**, 486 (1998).
[17] Radford, S. J. E. and Chamberlin, R. A., "Atmospheric transparency at 225 GHz over Chajnantor, Mauna Kea, and the South Pole," *ALMA Memo* **334.1** (2000).
[18] Radford, S., "Site characterization for mm/submm astronomy," *ASP Conf. Ser.* **266**, 148 (2002).
[19] Bornemann, J. and Labay, V. A., "Ridge waveguide polarizer with finite and stepped-thickness septum," *IEEE Trans. MTT* **43**, 95 (1995).
[20] Padin, S. et al., "The Cosmic Background Imager," *PASP* **114**, 83–97 (2002).
[21] Jarosik, N. et al., "Design, Implementation and Testing of the MAP Radiometers," *ApJS* **145**, 413 (2003).
[22] Leitch, E. et al., "Measurement of polarization with the Degree Angular Scale Interferometer," *Nature* **420**, 763–771 (2002).
[23] Hedman, M. M., Barkats, D., Gundersen, J. O., Staggs, S. T., and Winstein, B., "A Limit on the Polarized Anisotropy of the Cosmic Microwave Background at Subdegree Angular Scales," *Astrophys. J.* **548**, L111–L114 (2001).
[24] Barkats, D. et al., "CMB Polarimetry using Correlation Receivers with the PIQUE and CAPMAP Experiments," *ApJS* **159**, 1 (2005).
[25] Gaier, T. et al., "Amplifier arrays for CMB polarization," *New Astronomy Rev.* **47**, 1167–1171 (2003).
[26] Bogdan, M., Kapner, D., Samtleben, D., and Vanderlinde, K., "Digital control and data acquisition system for the QUIET experiment," *Nucl. Instrum. Methods Phys. Res., Sect. A* **572**(1), 338 – 339 (2007).